Supporting Information

Digital Light Processing 3D Printable Smart Silicone-based Elastomeric Composites based on a Synergistic Dual-compatibilization Strategy

Si-ying Lan, [a] *Fu-yue Tian,* [a] *Xin-yue Hao,* [a] *Xin-yu Li,* [b] *Jing Bai,* [b] *Nan-ying Ning,* [a, c, d] *Bing Yu,* [a, c, d, *] *Ming Tian* [a, c, d, *]

a State Key Laboratory of Organic–Inorganic Composites, Beijing University of Chemical Technology, Beijing 100029, China

b State Key Laboratory of Fluorine and Nitrogen Chemicals, School of Chemical Engineering and Technology, Xi'an Jiao Tong University, Xi'an, Shaanxi, 710049, China

c Beijing Advanced Innovation Center for Soft Matter Science and Engineering, Beijing University of Chemical Technology, Beijing 100029, China

d Key Laboratory of Carbon Fiber and Functional Polymers, Ministry of Education, Beijing University of Chemical Technology, Beijing 100029, China

*Corresponding author: tianm@mail.buct.edu.cn; yubing@mail.buct.edu.cn

Synthesis and structural characterization of amino-functionalized carbon quantum dots (NH_2-CDs)

(1) Synthesis of Amino-Terminated Polydimethylsiloxane (PDMS-NH_2): The synthetic route is illustrated in Scheme S1.

Based on the theoretical molecular weight (M_n = 2000 g/mol), the monomer-to-end-capper ratio was calculated. In a 250 mL three-neck flask, 100 g of octamethyl-1,3,5,7,2,4,6,8-tetraoxatetrasilocane (D4) and 0.25 g of N,N,N-Trimethyl-N-benzylammonium hydroxide catalyst were thoroughly mixed and heated to 50° C under vacuum to remove low-molecular-weight impurities until no further condensate was observed. The temperature was then raised to 80 °C, and 12.73 g of the amino-terminating agent 1,3-bis(3-aminopropyl)-1,1,3,3-tetramethyldisiloxane (BAPTDMS) was added. The reaction proceeded under a nitrogen atmosphere at 80 °C for 8 h. Subsequently, the temperature was increased to 170 °C to deactivate the catalyst N,N,N-Trimethyl-N-benzylammonium hydroxide, maintained for 10 min, and further elevated to 180 °C under reduced pressure to eliminate residual impurities and catalyst. The final product, designated PDMS-NH_2, was obtained with an actual yield of ~86%.

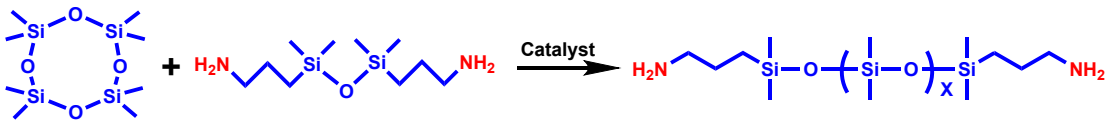

Scheme S1 Synthesis route of PDMS-NH_2

(2) Synthesis and characterization of amino-functionalized carbon quantum dots grafted with PDMS chains (NH_2-CDs): The synthetic route is illustrated in Scheme S2.

First, 10 mL of PDMS-NH_2 and 0.5 g of Citric Acid (CA) were poured into the liner of a hydrothermal reaction kettle. Subsequently, the reaction kettle was placed in a high-temperature oven and maintained at 180 °C for 6 h. After being allowed to cool to room temperature, a transparent yellow product was obtained. The product was then dissolved in petroleum ether and subjected to dialysis for 24 h to remove unreacted silicone oil residues. Once the petroleum ether in the carbon quantum dot solution was completely removed, the solution was transferred to a vacuum oven and dried at 50 °C for 6 h. Finally, amino-functionalized carbon quantum dots (designated as NH_2-CDs) were obtained as the target product.

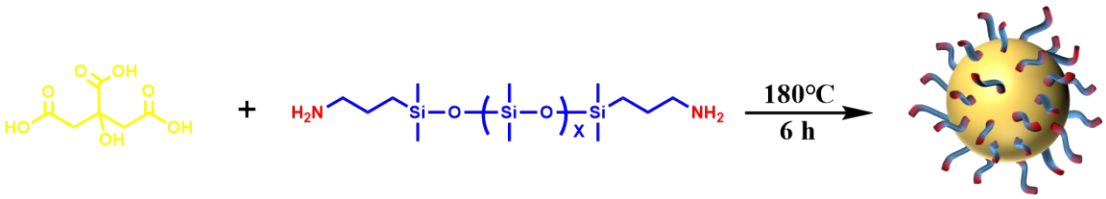

Scheme S2 Synthesis route of NH_2-CDs

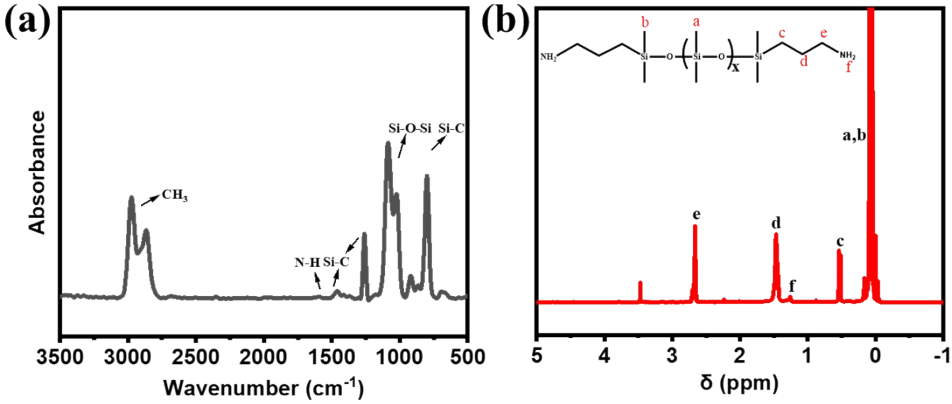

Figure S1 (a) FTIR spectra of PDMS-NH_2; (b) ^{1}H NMR spectrum of PDMS-NH_2

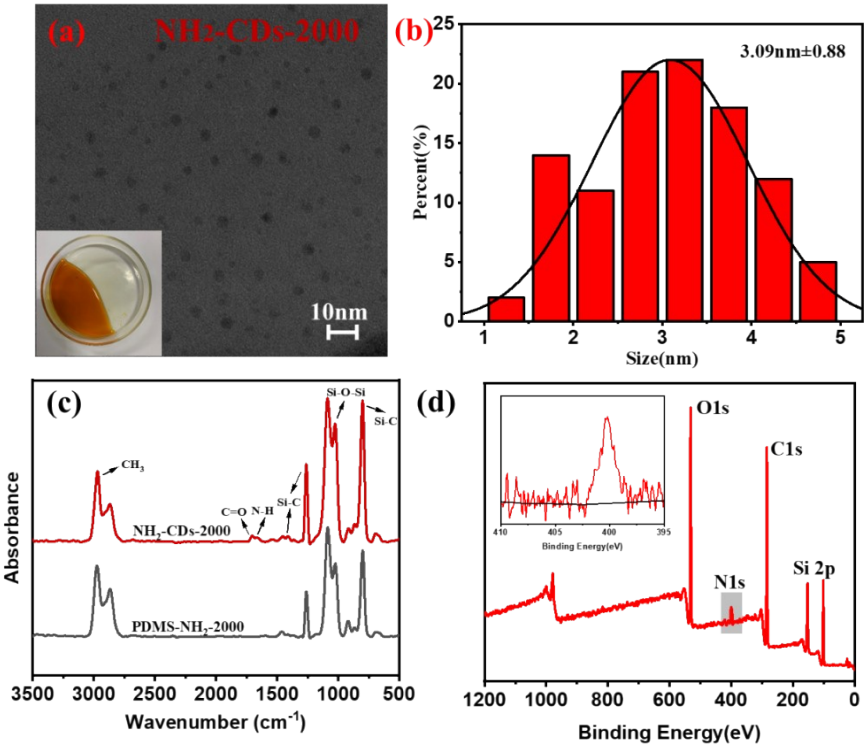

Figure S2 (a) The HRTEM micrograph of NH_2-CDs; (b) Statistical diagram of particle size distribution of NH_2-CDs (c) FTIR spectra of NH_2-CDs; (d) XPS of NH_2-CDs

From the high-resolution transmission electron microscopy (HRTEM) images and

size distribution histograms of NH_2-CDs, it can be observed that the product exhibits an average particle size of 3.09 ± 0.88 nm, with a nanospherical structure, a normal size distribution, and uniform particle dimensions. Meanwhile, Fourier transform infrared spectroscopy (FTIR) was used to conduct a structural comparison between PDMS-NH_2 and NH_2-CDs. A stretching vibration peak of C=O was observed at 1700 cm^{-1}, which confirms that the -COOH groups on the surface of the citric acid carbon core have reacted with the -NH_2 groups at the chain ends of PDMS-NH_2 to form amide bonds (-CO-NH-), indirectly verifying the successful synthesis of NH_2-CDs.

As inferred from the raw materials, NH_2-CDs is mainly composed of the elements O, N, C, and Si. X-ray photoelectron spectroscopy (XPS) analysis was performed on the product, revealing characteristic peaks of O 1s (532 eV), N 1s (399 eV), C 1s (285 eV), and Si 2p (154 eV and 102 eV). The characteristic peak of N 1s indicates that the N atoms on the surface of NH_2-CDs mainly exist in the forms of -NH_2 and -CO-NH-. Combined with the results of FTIR and XPS, the successful synthesis of NH_2-CDs is confirmed.

Synthesis and structural characterization of modified polycaprolactone (PCL-DA)

In a 150 mL single-neck flask, 10 g of polycaprolactone (PCL, 5×10^{-3} mol) was dissolved in 25 mL of dichloromethane (CH_2Cl_2) under magnetic stirring at 300 rpm. After complete dissolution, 2.33 g of isocyanato ethyl methacrylate (DA, 1.5×10^{-2} mol) and 0.1 mL (1 wt.% relative to PCL) of dibutyltin dilaurate (DBTDL) were added as the end-capping agent and catalyst, respectively. The flask was sealed to prevent solvent evaporation, and the reaction proceeded at room temperature for 48 h. The crude product was purified via precipitation in excess petroleum ether. The mixture was stirred for 5 min using a magnetic stir bar to remove unreacted reagents and impurities. This washing step was repeated for three times. The final product, a transparent and colorless viscous liquid (PCL-DA), was collected and vacuum-dried at room temperature, yielding ~98%.

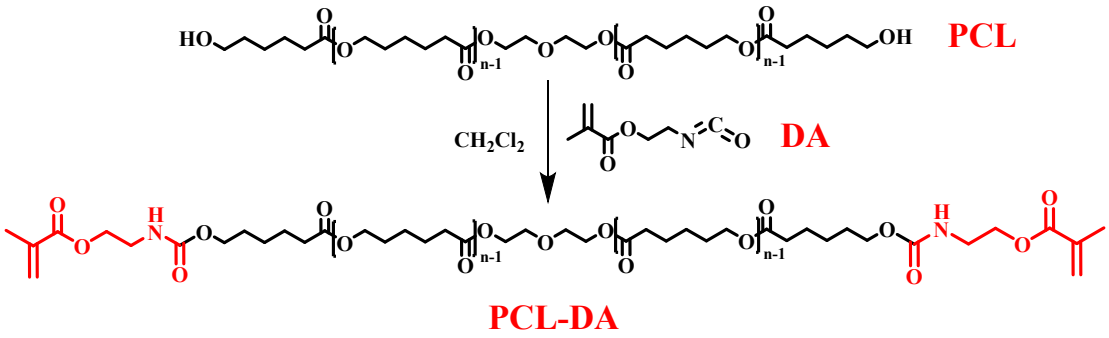

Figure S3 Synthesis route of PCL-DA

The hydroxyl (-OH) groups at both termini of polycaprolactone (PCL) react with the isocyanate (-N=C=O) groups of isocyanato ethyl methacrylate (DA) via nucleophilic addition, forming urethane linkages (-O-CO-NH-). Comparative analysis of the Fourier-transform infrared (FTIR) spectra of PCL, DA, and the modified PCL-DA reveals critical evidence for successful modification: the characteristic absorption peak of the -N=C=O group at 2270 cm^{-1} disappears in the PCL-DA spectrum, confirming the consumption of isocyanate groups through the nucleophilic reaction. Concurrently, the peak areas corresponding to out-of-plane C-H bending vibrations in the methacrylate moiety (observed at 585 cm^{-1}, 650 cm^{-1}, and 815 cm^{-1}) are significantly reduced. This reduction arises from the covalent attachment of methacryloxyethyl isocyanate to the high-molecular-weight PCL termini, which decreases the relative abundance of acrylate-associated C-H bonds. Together, these spectral changes validate the successful synthesis of PCL-DA, demonstrating the effective integration of methacrylate functionalities into the PCL structure.

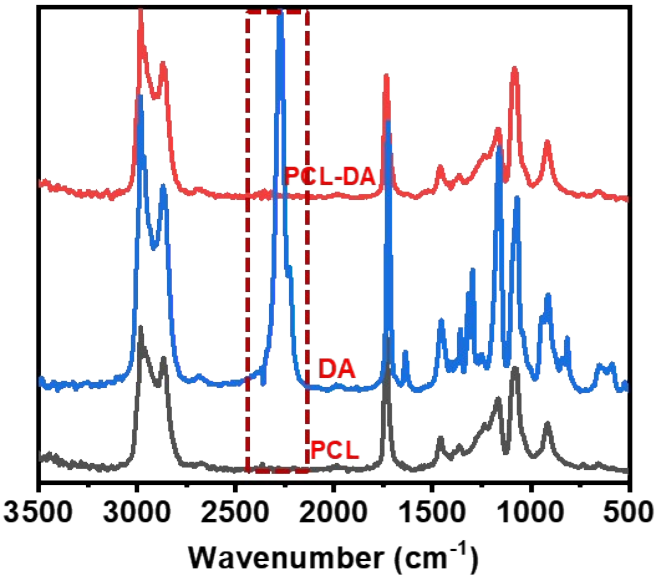

Figure S4 FTIR spectra comparison chart of PCL, DA, and PCL-DA

The NMR spectra of PCL and PCL-DA are shown in Figure S4. In the PCL-DA spectrum, characteristic peaks emerged at δ = 1.9 ppm (peak l, corresponding to methyl protons (-CH_3) in the methacryloyl group of DA), δ = 3.5 ppm (peak h, methylene protons (-CH_2-) adjacent to the urethane linkage (-O-CO-NH-CH_2-)), δ = 4.2 ppm (peak i, methylene protons (-CH_2-) bridging the amine group (-NH-CH_2-CH_2-)), and δ = 5.6/6.1 ppm (peaks j/k, vinyl protons (-CH_2=CH-) of the methacrylate moiety). The appearance of these peaks confirms the successful synthesis of PCL-DA. The bifunctional end-capping efficiency, calculated by integrating the peak area ratio between the methylene protons on the PCL backbone (peak f) and the methacrylate vinyl protons (peaks j/k), yielded an average value of ~75%, accounting for potential mono-end-capped or unreacted PCL chains. To further validate the presence of bifunctional groups, UV curing of PCL-DA mixed with photo-initiator TPO-L produced a transparent solid, confirming that a majority of PCL-DA retained dual methacrylate termini. This result aligns with the NMR-derived efficiency, supporting the reliability of the calculated end-capping rate as a reference for assessing functionalization efficacy.

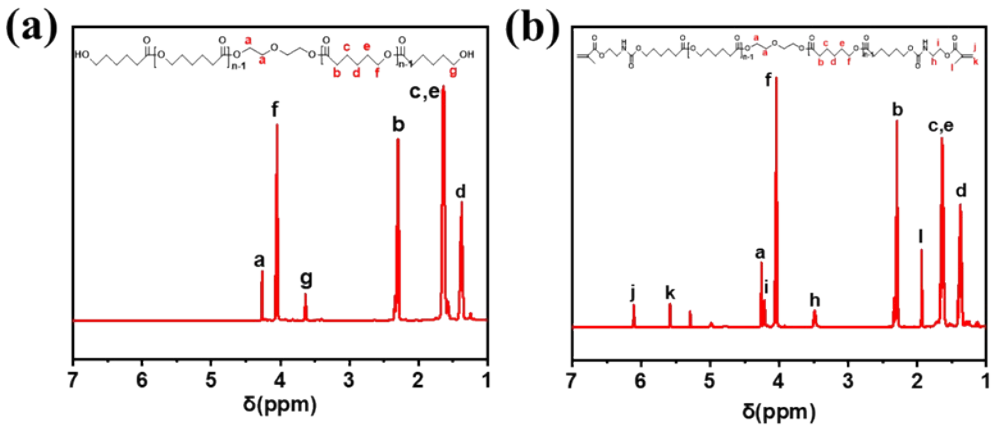

Figure S5 (a) ^{1}H NMR spectra of PCL; (b) ^{1}H NMR spectra of PCL-DA; Solvent: $CDCl_3$

Table S1 Peak position and integrated area

Chemical Shifts	Integral Area
b（δ=2.3 ppm）	7.65
c, e（δ=1.6 ppm）	15.99
d（δ=1.4 ppm）	7.77
f（δ=4.0 ppm）	7.89
h（δ=3.5 ppm）	2.05
i（δ=4.2 ppm）	2.07
j（δ=6.1 ppm）	1.00
k（δ=5.6 ppm）	1.00
l（δ=1.9 ppm）	3.04

Preparation of SiR/PCL/NH_2-CDs and SiR/PCL-DA/NH_2-CDs DLP Photocurable 3D-Printed Silicone Elastomeric composites

DLP 3D Printer Preprocessing: the resin tank of the DLP 3D printer was removed, followed by lowering and tightening the printing build plate to ensure close contact with the lower UV light panel; after which, build plate calibration was performed using the operating software. Subsequently, the uniformly mixed liquid precursor (with air bubbles removed) was poured into the resin tank, the printer cover was closed for light protection, and the dimensions of the printed part were set before slicing the modeled

component, with key slicing parameters including exposure time and slice layer thickness. Meanwhile, the first three sliced layers were set to a thickness of 0.075 mm with an exposure time of 8.5 s, while the subsequent sliced layers adopted a thickness of 0.1 mm with an exposure time of 7.5 s.

Post-processing of Printed Parts: the printed part was removed from the build plate, then soaked in an anhydrous ethanol solution for 2 min to remove residual precursor liquid from the part's surface. After being fished out and air-dried naturally, it was placed under a UV lamp with a wavelength of 405 nm and an intensity of 30 mW/cm^2 for 60 s to achieve complete curing.

In-Situ FTIR analysis of two-component silicone elastomeric composite materials (SiR/PCL-DA/NH_2-CDs)

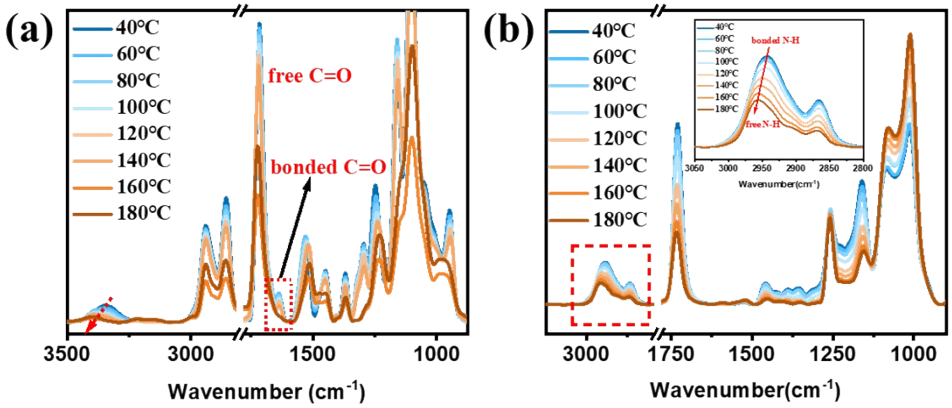

Figure S6 (a) In-Situ FTIR of PCL-DA; (b) In-Situ FTIR of SiR/PCL-DA/NH_2-CDs

The molecular structure of PCL-DA suggests the presence of N-H and C=O bonds, enabling intermolecular hydrogen bonding. Temperature-dependent *In-Situ* FTIR analysis of PCL-DA revealed dynamic hydrogen bond behavior: as temperature increased, the hydrogen-bonded N-H stretching vibration (bonded N-H) at 3340 cm^{-1} progressively shifted to higher wavenumbers, transitioning to free N-H, while the hydrogen-bonded C=O peak (bonded C=O) at 1637 cm^{-1} similarly shifted and merged into the free C=O peak at 1718 cm^{-1}. This observation confirms the prevalence of hydrogen bonds in PCL-DA. Using the same methodology, hydrogen bonding in the SiR/PCL-DA/NH_2-CDs system was investigated. *In-Situ* FTIR analysis demonstrated

that the intensity of bonded N-H gradually decreased with rising temperature, accompanied by an increase in free N-H signals, whereas the hydrogen-bonded C=O exhibited minimal variation. Given that both PCL-DA and NH_2-CDs possess N-H and C=O functionalities, these results confirm hydrogen bonding interactions between NH_2-CDs and PCL-DA, providing a molecular-level rationale for the enhanced compatibilization effect of NH_2-CDs in the SiR/PCL-DA blend.

Mechanical properties of two-component organosilicon elastomeric composite materials (SiR/PCL/NH_2-CDs and SiR/PCL-DA/NH_2-CDs)

As shown in Table 1, the raw SiR sample exhibits relative insufficient mechanical performance, with a tensile strength of 350.0 kPa, an elongation at break of 290%, a fracture energy of 59.7 $kJ \cdot m^{-3}$, an elastic hysteresis of 157.2 $kJ \cdot cm^{-3}$, and a permanent set of 2.21%. When PCL is introduced to form the SiR/PCL composite, poor compatibility between SiR and PCL leads to weak interfacial interactions and severe chain slippage, causing a significant deterioration in mechanical performance: the tensile strength decreases to 226.5 kPa, the elongation at break decreases to only 156%, the fracture energy plummets to 22.9 $kJ \cdot m^{-3}$, while the elastic hysteresis surges to 1795.4 $kJ \cdot cm^{-3}$ and the permanent set rises to 11.27%. Upon introducing the amphiphilic block copolymer PU-*co*-PSi, it acts as a compatibilizer by forming physical entanglements with SiR domains and hydrogen bonds with PCL domains at the interface, restricting chain slippage and restoring and improving performance: the tensile strength of SiR/PCL/PU-*co*-PSi increases to 361.5 kPa (exceeding that of pure SiR), the elongation at break increases to 309%, the fracture energy rises to 70.0 $kJ \cdot m^{-3}$, and both the elastic hysteresis and permanent set decrease to 1712.0 $kJ \cdot cm^{-3}$ and 4.95%, respectively. Further addition of NH_2-CDs induces a nanoconfinement effect via Pickering adsorption at the interface, constraining local chain mobility and enhancing hydrogen bond-mediated stress transfer, thus enabling SiR/PCL/NH_2-CDs to show further improvements: the tensile strength, elongation at break, and fracture energy increase to 408.2 kPa, 336%, and 85.8 $kJ \cdot m^{-3}$, while the elastic hysteresis decreases to 1497.0 $kJ \cdot cm^{-3}$ (with the permanent set slightly rising to 5.62%). Finally, when methacrylate groups (DA) are introduced at the end of PCL in combination with NH_2-

CDs, UV-triggered interfacial co-crosslinking between SiR and PCL synergizes with compatibilization and the nanoconfinement effect, allowing SiR/PCL-DA/NH_2-CDs to achieve the optimal mechanical performance: a tensile strength of 440.7 kPa, an elongation at break of 367%, a fracture energy of 101.9 $kJ \cdot m^{-3}$, and the elastic hysteresis remains relatively low at 1567.8 $kJ \cdot cm^{-3}$ with the permanent set controlled at 5.53%.

As shown in Table S2, the glass transition temperature of the SiR phase ($T_{g,\ SiR}$), the PCL phase ($T_{g,\ PCL}$), and the temperature difference between the two phases (ΔT_g) determined by DMA are exhibited. The $T_{g,\ SiR}$ shows minimal variation across samples (ranging from -113.9 °C for SiR/PCL/PU-*co*-PSi to -113.4 °C for SiR/PCL/NH_2-CDs and -113.5 °C for SiR/PCL-DA/NH_2-CDs), indicating the SiR phase's thermal transition is relatively unaffected by these modifiers. In contrast, $T_{g,\ PCL}$ exhibits a clear downward trend: from -34.9 °C (with PU-*co*-PSi) to -35.3 °C (with NH_2-CDs) and further to -38.8 °C (with PCL-DA + NH_2-CDs), while ΔT_g also decreases sequentially (from 79.0 °C to 78.1 °C and then 74.7 °C). A reduced ΔT_g signifies enhanced compatibility between SiR and PCL: PU-*co*-PSi first improves compatibility via interfacial entanglements and hydrogen bonding, NH_2-CDs then reinforce interfacial interactions through Pickering adsorption to lower $T_{g,\ PCL}$, and shrink ΔT_g, and finally, modifying PCL with methacrylate groups (DA) alongside NH_2-CDs enables UV-triggered co-crosslinking, maximizing interfacial adhesion and resulting in the lowest $T_{g,\ PCL}$ and ΔT_g, thus achieving the best phase compatibility among all samples.

Table S2 The DMA data of the two-component silicone elastomeric composite material

Simple name	$T_{g,\ SiR}$ /°C	$T_{g,\ PCL}$ /°C	ΔT_g/°C
SiR/PCL/PU-*co*-PSi	-113.9	-34.9	79.0
SiR/PCL/NH_2-CDs	-113.4	-35.3	78.1
SiR/PCL-DA/NH_2-CDs	-113.5	-38.8	74.7

Thermal stability performance analysis of two-component organosilicon elastomeric composite materials (SiR/PCL/NH_2-CDs and SiR/PCL-DA/NH_2-CDs)

Thermogravimetric analysis (TGA) of pure SiR and pure PCL revealed distinct

degradation stages: the first weight-loss step corresponds to the thermal decomposition of the PCL phase, while the second step is attributed to the degradation of flexible SiR chains. Upon incorporating compatibilizers, the thermal decomposition temperatures at 30 wt.% and 70 wt.% mass loss increased across both phases, indicating enhanced thermal stability of the blended system. Notably, NH_2-CDs exhibited superior efficacy over the industrial compatibilizer PU-*co*-PSi in improving thermal stability. This enhancement is further amplified in the SiR/PCL-DA/NH_2-CDs system, where covalent crosslinking structures between the phases confer exceptional thermal resistance compared to the SiR/PCL/NH_2-CDs system.

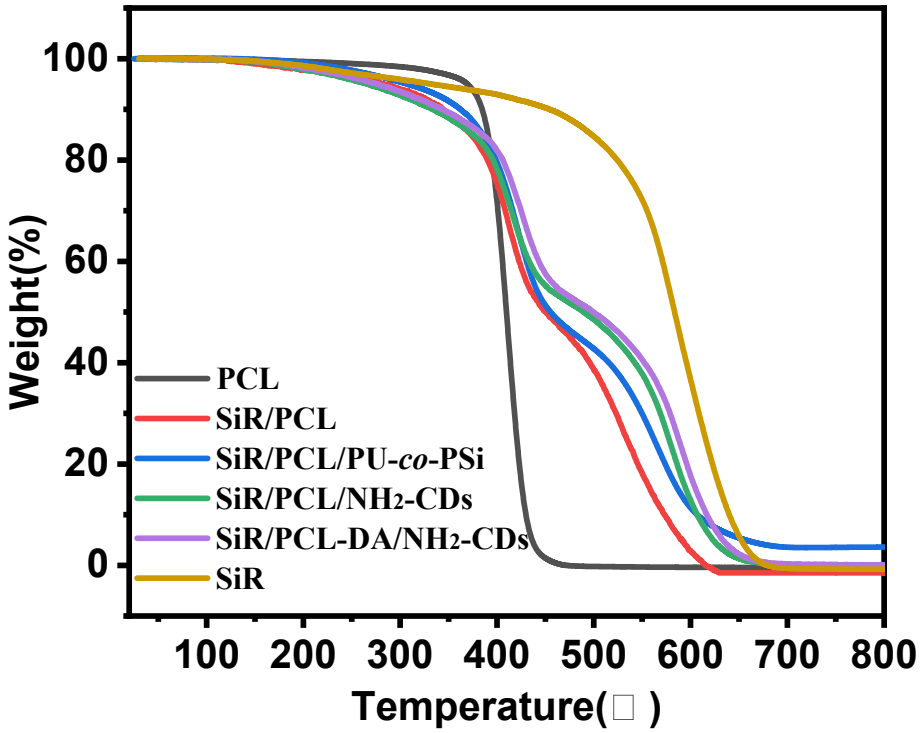

Figure S7 TGA curves of two-component silicone elastomeric composite material

Table S3 Thermal stability data of two-component silicone elastomeric composite material

Simple Name	30 wt.% thermal decomposition temperatures /°C	70 wt.% thermal decomposition temperatures /°C	Residual mass /wt.%
SiR/PCL	408.5	523.0	0

SiR/PCL/PU-*co*-PSi	416.1	549.6	3.60
SiR/PCL/NH_2-CDs	414.8	568.6	0.08
SiR/PCL-DA/NH_2-CDs	423.7	578.7	0.10

Viscosity analysis of two-component organosilicon elastomeric composite materials (SiR/PCL-DA/NH_2-CDs)

Figure S8 depicts the curves of dynamic viscosity variation with curing time for the SiR/PCL-DA/NH_2-CDs composite. To improve processability and ensure uniform dispersion of components, tetrahydrofuran (THF) was initially introduced, resulting in a low initial viscosity of 222.96 mPa • s. As the curing process proceeds, the system undergoes cross-linking reactions, inducing a rapid increase in viscosity. Notably, the viscosity surges sharply within approximately 30 s and eventually stabilizes at a maximum value of 436290 mPa • s, indicating that the composite completes curing within 30 s and forms a dense cross-linked network. This rapid and significant viscosity growth reflects the high efficiency of cross-linking between SiR and PCL-DA in the presence of NH_2-CDs: NH_2-CDs not only enhance interfacial compatibility between phases but also synergistically promote the curing reaction (e.g., UV-triggered co-crosslinking), enabling the system to rapidly transition from a processable low-viscosity state to a cured high-viscosity state. The final high cured viscosity (4.36×10^5 mPa • s) also confirms the formation of a robust cross-linked network, which is beneficial for improving the mechanical and other properties of the composite.

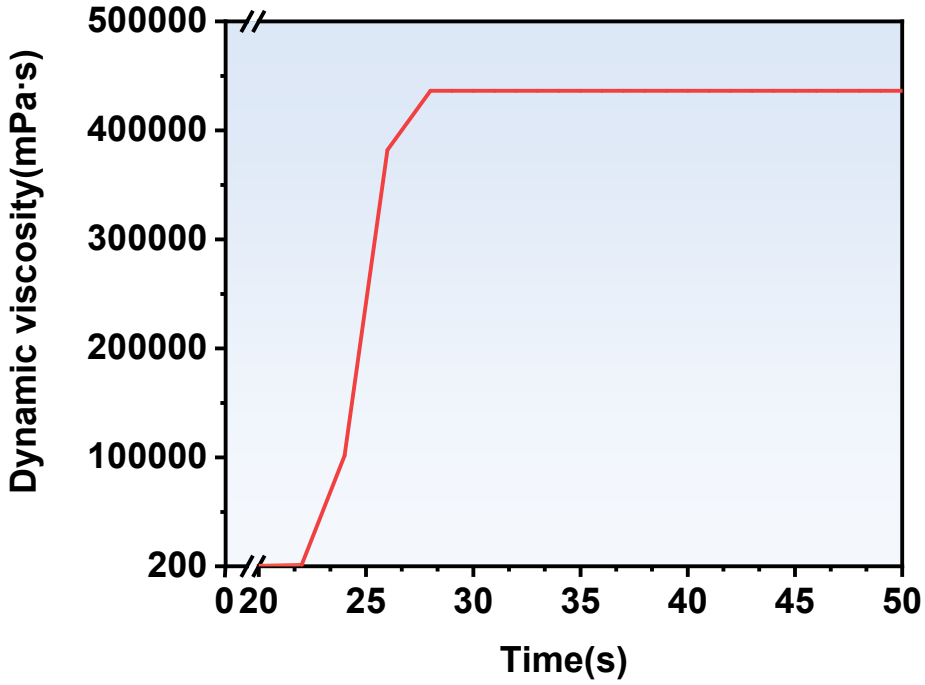

Figure S8 Curves of viscosity variation with curing time of SiR/PCL-DA/NH_2-CDs

Shape Recovery and Structure Change of SiR/PCL-DA/NH_2-CDs Composite during Heating and Cooling

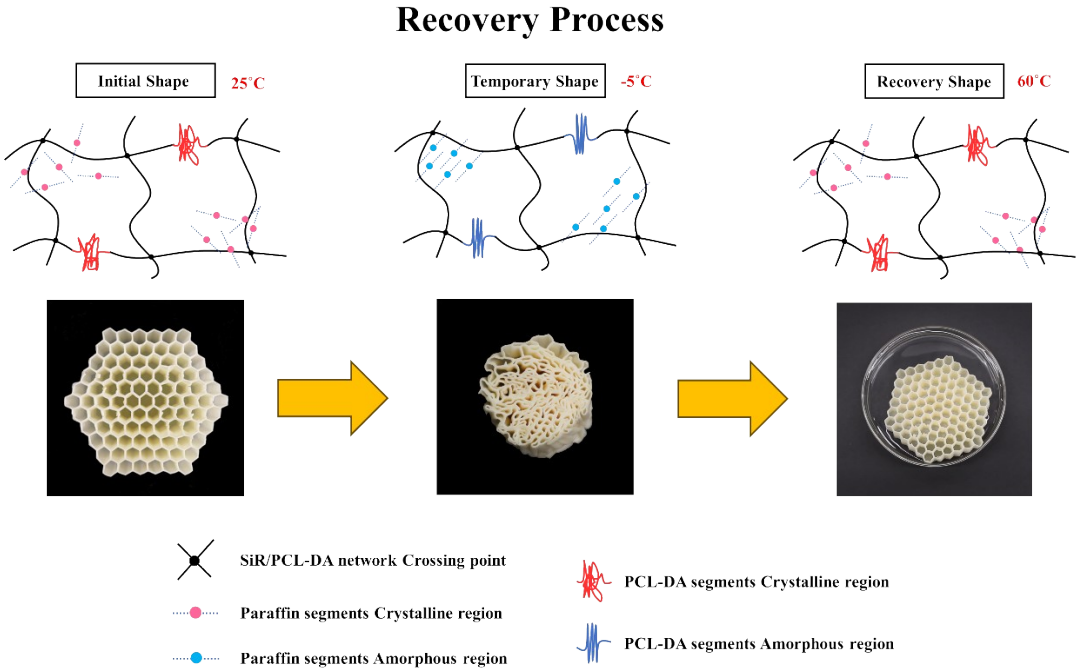

Figure S9 Illustration of the structure change of SiR/PCL-DA/NH_2-CDs during heating and cooling

This study elucidates the multi-stage phase transition-driven mechanism underlying the thermally induced shape memory behavior of the SiR/PCL-DA/NH_2-CDs composite system through DSC and XRD characterization. DSC results revealed that the incorporation of compatibilizers and the modification of PCL induced a heterogeneous crystalline distribution in the PCL phase. Consequently, the shape memory transition temperature (T_t) and fixation temperature (T_f) were determined as 60°C and -5°C, respectively. During the shape fixation stage ($T = T_f$), externally applied forces prompted conformational rearrangement of PCL chains, forming a highly ordered β-crystalline structure. Simultaneously, the covalent crosslinking network and nanoparticle-mediated physical entanglement synergistically locked the temporary deformation. Upon heating to T_t, the metastable micro-crystallites melted first, restoring local chain mobility, followed by the dissociation of stable crystalline domains, which triggered entropy-driven network retraction to achieve shape recovery. This process adheres to a "dual-phase synergy" mechanism: the covalent/physical crosslinking network serves as the stabilizing phase to retain the permanent shape, while the reversible melting-recrystallization of PCL crystalline domains acts as the thermally responsive reversible phase for temporary shape fixation.